

# Development of a Discrete-Time Map for Nonlinear Analysis of Flyback Converter

David E. Giraldo-Hernández<sup>1,\*</sup>, Mario A. Bolaños-Navarrete<sup>1</sup>, Fabiola Angulo<sup>1</sup>, Gustavo Osorio<sup>1</sup>, Nicols Astaiza<sup>2</sup>, Juan David Mina-Casaran<sup>2</sup>, and Wilder Herrera<sup>2</sup>

<sup>1</sup> Department Ingeniería Eléctrica, Electrónica y Computación,

Universidad Nacional de Colombia - Sede Manizales, Manizales, Colombia

<sup>2</sup> Rynova Research Group, Rymel Ingeniería Eléctrica S.A.S., Copacabana, Colombia

Email: dgiraldohe@unal.edu.co (D.E.G.-H.), mabolanosn@unal.edu.co (M.A.B.-N.), fangulog@unal.edu.co (F.A.),

gaosoriol@unal.edu.co (G.O.), joveninvestigador2@rymel.com.co (N.A.),

direccioninnovacion@rymel.com.co (J.D.M.-C.), Wilderherrera@rymel.com.co (W.H.)

Manuscript received November 18, 2024; revised January 24, 2025; accepted February 6, 2025

\*Corresponding author

**Abstract**—This paper presents a discrete-time map calculated from the nonlinear averaged model for a flyback DC-DC converter with peak current control. Traditional switched models, although accurate, are computationally expensive, limiting their practicality for rapid analysis. To address this limitation, we propose a novel discrete-time map of the flyback converter. The model achieves a simulation time reduction of over 97% compared to event-driven models while preserving high accuracy in both transient and steady-state conditions, with errors of less than 1%. Numerical simulations validate the model's performance and its ability to predict system responses to perturbations effectively. This method enables precise detection of transitions between Continuous Conduction Mode (CCM) and Discontinuous Conduction Mode (DCM). This feature provides an advantage over standard averaged models by simplifying mode detection and improving computational efficiency. This approach is particularly useful for applications in renewable energy and power electronics. Future work will focus on integrating this model into real-time simulation environments to enhance control strategies.

**Index Terms**—continuous conduction mode, discontinuous conduction mode, discrete-time map, flyback, peak current mode control, power converter

## I. INTRODUCTION

A power converter modifies electrical energy levels by using inductors, capacitors, and components like MOSFETs, transistors, and diodes [1]. These devices are prevalent globally, as many products and appliances depend on converters to process energy in various fields, such as photovoltaic applications [2], aerospace applications [3], electric vehicle chargers [4], battery chargers [5], and solid-state lighting [6]. One of the key power converters is the flyback converter, recognized for its high voltage gain and the electrical isolation between its primary and secondary windings. This isolation is especially advantageous for applications in renewable energy, where safety and efficiency are crucial.

The most accurate representation of a converter typically involves switched models, which effectively replicate nonlinear behaviors [7]. While these models are

precise in simulating transient and steady-state responses, they often lead to longer simulation times and higher computational demands [8], limiting their use. In applications like output voltage control, however, switching details are less critical [9], making computationally efficient models an attractive alternative.

Discrete maps have been extensively used to analyze the dynamics of power converters, particularly in studying the transition between Continuous Conduction Mode (CCM) and Discontinuous Conduction Mode (DCM). Reference [10] investigated the existence conditions of limit cycles and stability loss in an open-loop DC-DC boost converter with a constant power load operating in DCM using a piecewise smooth map. Reference [11] provided a comprehensive classification of discrete-time models for analyzing nonlinear phenomena in DC-DC converters, covering various topologies and control modes. The practical implications of CCM and DCM operations were experimentally compared in [12] for flyback converters, examining aspects such as component stress, voltage regulation, and efficiency. Reference [13] demonstrated the feasibility of using discrete-map models for stability analysis of voltage-mode DC-DC converters in CCM, specifically applying this approach to buck converters. These studies collectively highlight the effectiveness of discrete maps in enhancing the understanding of power converter dynamics across different operational modes.

Discrete-time modeling is a powerful approach for analyzing power converters, offering insights into stability, performance, and nonlinear behavior [14]. This method represents converters as discrete dynamical systems evolving through iterative processes, where each new state depends on the current state [15, 16]. By sampling continuous-time variables at regular intervals, it creates a mapping or difference equation connecting state vectors at the beginning and end of each period [17]. This technique effectively captures nonlinear and chaotic characteristics, enabling more accurate analysis of converter performance [11, 18]. Discrete-time modeling can accommodate variations in circuit parameters and parasitic resistances, which are often neglected in traditional approaches. It also

provides a basis for developing analytical compensators and assessing robust stability [15].

Discrete maps are particularly effective for modeling transitions between operational modes, such as CCM and DCM [19]. They excel in analyzing bifurcations and chaotic behaviors, providing detailed insights into system stability and responses to perturbations [20]. One of the key advantages of discrete maps is their computational efficiency; they operate significantly faster than traditional switched models, which generally require extensive computational resources and longer simulation times [21].

In contrast, averaged models simplify system analysis by averaging over a complete switching cycle. This approach reduces computational time and streamlines the modeling process, making it efficient for capturing low-frequency behaviors. These characteristics make them very valuable for applications where computational efficiency is paramount [22].

Both discrete maps and averaged models offer significant advantages over traditional switched models in terms of speed and efficiency, making them indispensable tools for power electronics analysis.

In this context, the present work combines the advantages of the averaged model and discrete-time map by developing a discrete map model for the flyback converter, derived from its nonlinear averaged model and validated through numerical simulations using the conventional switched model. This approach enables accurate identification of transitions between CCM and DCM through the use of the valley current. Additionally, it significantly reduces simulation time—by more than 97%—and computational requirements, while maintaining high accuracy in both transient and steady-state conditions. These features make it a powerful tool for analyzing and optimizing power converter performance in renewable energy applications.

The structure of this paper is as follows: Section II provides an overview of the system under investigation, specifically a DC-DC flyback. Section III delves into the detailed modeling of the converter, focusing on the derivation of the discrete map model. In Section IV, the proposed discrete map is validated by comparing its performance against that of the traditional switched model. Finally, Section V present conclusions and future work.

## II. FLYBACK CONVERTER

The flyback converter, illustrated in Fig. 1, is a DC-DC converter consisting of a power supply  $v_{in}$ , a MOSFET  $S$ , a load resistor  $R$ , a capacitor  $C$ , the magnetizing inductance  $L_m$ , and a turns ratio  $n = N_1/N_2$ . The flyback converter provides isolation between the input and output, making it widely used due to its high voltage gain and the isolation it offers between the source and the load through the use of coupled coils or a potential transformer [23]. Among its main features and advantages are its efficiency, reliability, fast response, simple structure, low cost, and compact size, all of which contribute to ease and simplicity in control design [24–27].

Similar to other converters, the behavior of the current is crucial in the flyback converter, specifically the magnetizing current  $i_{L_m}$ . This current is related to the

primary-side current  $i_{prim}$  and the secondary-side current  $i_D$  which is the same of the diode, as shown:

$$i_{L_m} = i_{prim} + \frac{i_D}{n} \quad (1)$$

As in other converters, when  $i_{L_m} > 0$ , the system operates in CCM, and when  $i_{L_m} = 0$ , it operates in DCM.

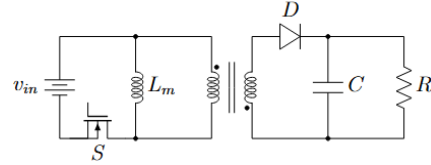


Fig. 1. Model of flyback converter.

### A. CCM Operation

Fig. 2 illustrates the behavior of the magnetizing current  $i_{L_m}$  in CCM, where the system operates through two topologies as shown in Fig. 3. Now, Fig. 3 (a) represents Topology T1 and Fig. 3 (b) represents Topology T2. The state variables in this system are the capacitor voltage  $v_C$  and the magnetizing current  $i_{L_m}$ .

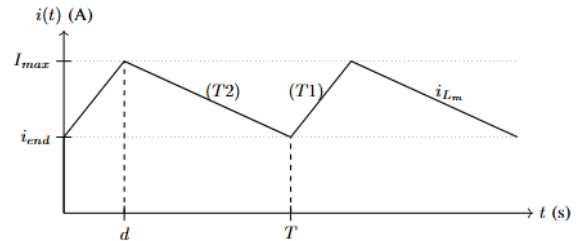


Fig. 2. Current  $i_{L_m}$  in CCM.

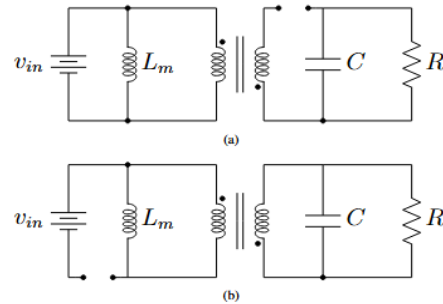


Fig. 3. Topology: (a) T1 and (b) T2.

In Topology T1, the MOSFET is closed, allowing current to flow through the primary winding, which causes energy to be stored in  $L_m$  and increases the magnetizing current  $i_{L_m}$ . However, since the diode is reverse-biased, no current flows to the secondary winding. Simultaneously, the capacitor supplies the load, discharging in the process. The equations governing the system's behavior in this topology are given by [25]:

$$\dot{v}_C = -\frac{v_C}{RC} \quad (2a)$$

$$i_{L_m} = \frac{v_{in}}{L_m} \quad (2b)$$

Subsequently, the MOSFET opens, and the system

switches to Topology T2. In this mode, the diode becomes forward-biased, allowing all the energy stored in  $L_m$  to be transferred to the secondary side. In this case, the current  $i_{L_m}$  begins to decrease while the current  $i_D$  starts to flow, charging the capacitor and supplying the load. The equations representing the system dynamics in this topology are in [25]:

$$\dot{v}_C = -\frac{v_C}{RC} + n \frac{i_{L_m}}{C} \quad (3a)$$

$$i_{L_m} = -n \frac{v_C}{L_m} \quad (3b)$$

### B. DCM Operation

When the system operates in DCM, it indicates that the magnetizing current  $i_{L_m}$  has reached zero, as shown in Fig. 4. In DCM, the system transitions through the two topologies described are like the ones described in CCM, but additionally enters a third Topology T3. In this mode, the MOSFET is open, and the diode is reverse-biased, as illustrated in Fig. 5, leaving only an RC circuit that discharges the capacitor. The equations describing the behavior of Topology T3 can be found in [25]:

$$\dot{v}_C = -\frac{v_C}{RC} \quad (4a)$$

$$i_{L_m} = 0 \quad (4b)$$

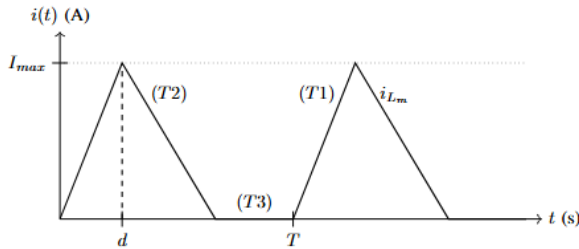


Fig. 4. Current  $i_{L_m}$  in DCM.

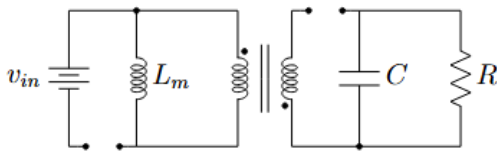


Fig. 5. Topology T3.

## III. DISCRETE-TIME MAP

To calculate the discrete-time map for flyback converter, a mathematical analysis and development of the system must be carried out, taking into account its mode of operation.

### A. CCM Solution

Since in CCM the magnetizing current  $i_{L_m}$  never reaches zero, and assuming each period is considered in isolation, with  $t \in (0, T)$ , the solution for the first Topology T1 is given by:

$$v_C(t) = e^{-\frac{t}{RC}} v_C(0) \quad (5a)$$

$$i_{L_m}(t) = \frac{v_{in}}{L_m} t + i_{L_m}(0) \quad (5b)$$

The duty cycle  $d$  corresponds to the time during which the MOSFET remains closed, which is valid until  $i_{L_m}$  reaches  $I_{max}$ . Since the system operates in CCM,  $i_{L_m}(0) \neq 0$ , and the time  $d$  can be calculated as follows:

$$d = (I_{max} - i_{L_m}(0)) \frac{L_m}{v_{in}} \quad (6)$$

Thus, at  $t = d$ , the voltage across the capacitor and the magnetizing current are given by:

$$v_C(d) = e^{-\frac{d}{RC}} v_C(T) \quad (7a)$$

$$i_{L_m}(d) = I_{max} \quad (7b)$$

In the next phase, it must be ensured that the system operates in CCM. For this reason, a  $\Delta_{num}$  is calculated, which represents the time at which the current reaches zero.

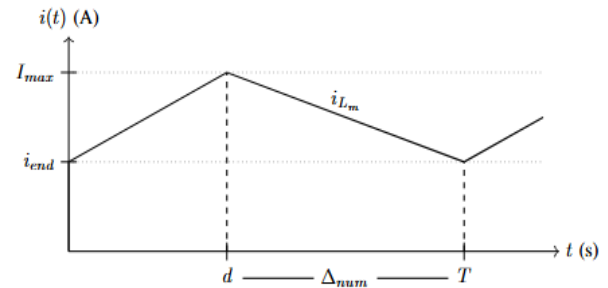


Fig. 6. CCM  $\Delta_{num}$ .

From Fig. 6, it can be seen that  $d + \Delta_{num} > T$ . Thus,  $\Delta_{num}$  is assigned as  $T - d$ , which corresponds to a known value. Now, assuming that the current slope is linear, it follows that:

$$i_{end} = I_{max} - n v_C \frac{\Delta_{num}}{L_m} \quad (8)$$

From (8), the value of  $i_{end}$  can be determined numerically. Similarly, the function that defines the time interval  $\Delta_{fun}$  (the same time interval as  $\Delta_{num}$  in Fig. 6) is expressed as:

$$\Delta_{fun} = \frac{L_m(I_{max} - i_{end})}{n v_C} \quad (9)$$

Now, the average value of the magnetizing current is given for the following expression:

$$\bar{i}_{L_m} = (I_{max} + i_{end}) \frac{\Delta_{fun}}{2 \Delta_{num}} \quad (10)$$

By substituting (9) into (10), the average value is given by:

$$\bar{i}_{L_m} = L_m \frac{I_{max}^2 - i_{end}^2}{2 n v_C \Delta_{num}} \quad (11)$$

Thus, by substituting (11) into equation (3a), we obtain:

$$\dot{v}_C = -\frac{v_C}{RC} + L_m \frac{I_{max}^2 - i_{end}^2}{2 C v_C \Delta_{num}} \quad (12)$$

The solution to this equation is represented by:

$$v_C(t) = \sqrt{e^{-\frac{2t}{RC}} v_C^2(d) + \frac{(I_{max}^2 - i_{end}^2) L_m R}{2 \Delta_{num}} \left(1 - e^{-\frac{2t}{RC}}\right)} \quad (13)$$

Finally, this expression is evaluated at  $T$ , and the initial condition for the next cycle is set, allowing the map  $x((k+1)T) = f(x(kT))$  to be obtained.

### B. DCM Solution

Given that  $i_{L_m}$  reaches zero, the solutions to the equations in Topology T1 are

$$v_C(t) = e^{-\frac{t}{RC}} v_C(0) \quad (14a)$$

$$i_{L_m}(t) = \frac{v_{in}}{L_m} t + i_{L_m}(0) \quad (14b)$$

Since the system operates in DCM,  $i_{L_m}(0) = 0$ , and based on the behavior during T1, the time  $d$  is determined as follows:

$$d = I_{max} \frac{L_m}{v_{in}} \quad (15)$$

Thus, at  $t = d$ , the voltage across the capacitor and the magnetizing current are given by:

$$v_C(d) = e^{-\frac{d}{RC}} v_C(0) \quad (16a)$$

$$i_{L_m}(d) = I_{max} \quad (16b)$$

In the next phase, the MOSFET opens and the current flowing through the secondary is proportional to the magnetizing current ( $i_D = n i_{L_m}$ ). Assuming that the capacitor discharges very little, the slope of the magnetizing current can be approximated as a constant, given by (3b). With this assumption, the time  $\Delta_{num}$ , which the current takes to reach zero, can be calculated as shown in Fig. 7.

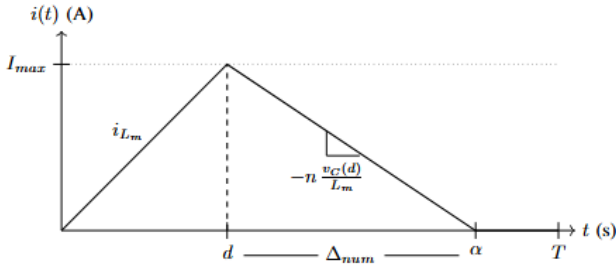


Fig. 7. DCM  $\Delta_{num}$ .

From Fig. 7, it can be observed that  $\Delta_{num}$  is represented by:

$$\Delta_{num} = \frac{I_{max} L_m}{n v_C(d)} \quad (17)$$

For the system to operate in DCM, it must be ensured that  $d + \Delta_{num} := \alpha \leq T$ . Similar to CCM, the expression for the crossing time  $\Delta_{fun}$  is determined as a function of constants and voltage, given by:

$$\Delta_{fun} = \frac{I_{max} L_M}{n v_C} \quad (18)$$

Similar to CCM, the average value of the magnetizing current in the secondary is determined by:

$$\bar{i}_{L_m} = I_{max} \frac{\Delta_{fun}}{2 \Delta_{num}} \quad (19)$$

By substituting (18) into this expression, we obtain:

$$\bar{i}_{L_m} = L_m \frac{I_{max}^2}{2 n v_C \Delta_{num}} \quad (20)$$

By substituting (20) into equation (3a), the result is:

$$\dot{v}_C = -\frac{v_C}{RC} + \frac{I_{max}^2 L_M}{2 C v_C \Delta_{num}} \quad (21)$$

The solution of which is given by:

$$v_C(t) = \sqrt{e^{-\frac{2t}{RC}} v_C^2(d) + \frac{I_{max}^2 L_M R}{2 \Delta_{num}} \left(1 - e^{-\frac{2t}{RC}}\right)} \quad (22)$$

With this expression,  $v_C(\alpha)$  is calculated, and it is established that  $i_{L_m}(\alpha) = 0$ . Finally, in the last phase,  $v_C(T)$  and  $i_{L_m}$  are recalculated as indicated:

$$v_C(T) = e^{-\frac{\alpha}{RC}} v_C(\alpha) \quad (23a)$$

$$i_{L_m}(T) = 0 \quad (23b)$$

With these analytical expressions, the map  $x((k+1)T) = f(x(kT))$  is constructed.

## IV. SIMULATION AND RESULTS

### A. System Response

The voltage and current responses of the exact event-driven model developed in MATLAB® and the discrete-time map were simulated and evaluated. The parameters used for evaluating the map are listed in Table I.

TABLE I: TYPE SIZES FOR CAMERA-READY PAPERS

Component / Parameter	Value
Input voltage ( $v_{in}$ )	12 V
Turns ratio ( $n = N_1/N_2$ )	1/30
Magnetizing inductance ( $L_M$ )	9.85 $\mu$ H
Period ( $T$ )	42.6 $\mu$ s
Capacitor ( $C$ )	30 $\mu$ F
Load resistance ( $R$ )	100 $\Omega$
Peak current ( $I_{max}$ )	15.7804 A

Initially, by comparing the simulation times between both models, it was found that the event-driven model took 4.188350 seconds, while the discrete-time map took 0.013017 seconds. The significant advantage of using the map is evident, as the simulation time was reduced by approximately 97%.

Fig. 8 shows the voltage response of the discrete-time map compared to the event-driven model. The greatest error, 45%, occurs during the initial iterations of the transient state. However, at  $t = 0.8$  ms, the error decreases to 10%, and at  $t = 0.005$  s (still in the transient state), the error is 0.8%. In the steady state, the error is less than 0.05%. Specifically, in the zoomed-in area, the error is 0.003%.

Fig. 9 shows the current response of the discrete-time map compared to the event-driven model. It can be seen that the maximum error is 1.38% at  $t = 0.6$  ms. Subsequently, at  $t = 4$  ms, the error decreases to 0.5%. Finally, from  $t = 10$  ms onward, the error remains below 0.1%. In the zoomed-in interval, the error is approximately 0.05%.

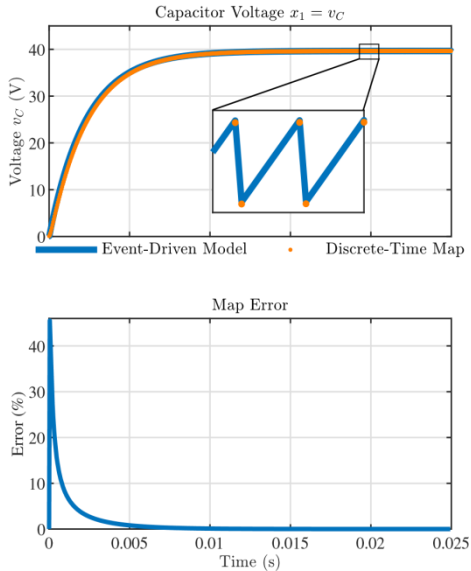


Fig. 8. Voltage response of the model.

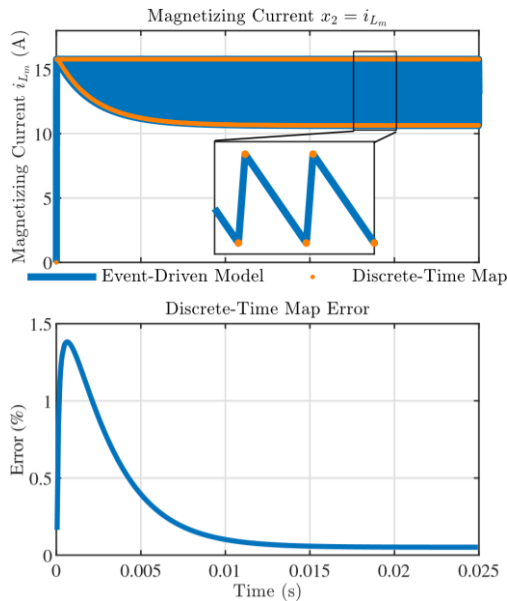


Fig. 9. Current response of the model.

### B. Response to Disturbances

To evaluate the robustness and responsiveness of the map against abrupt changes in operating conditions, simulations were conducted by introducing disturbances in the current reference. Initially, the reference current was perturbed from 15.7804 A to 13 A at 0.03 s, then increased to 30 A at 0.06 s. Finally, at 0.09, both the reference and the load were perturbed simultaneously, to 25 A 60  $\Omega$ , respectively.

Regarding simulation times, the event-driven model took 12.759044 seconds, while the discrete-time map took 0.028437 seconds. This represents an approximate reduction of 99.78% in simulation time.

Fig. 10 shows the voltage response of the models to perturbations. In this case, during the first transient, the maximum error of 45% occurs at  $t = 0.04$  ms. Following this, as shown in the zoomed-in view, the highest error peaks appear during reference changes; however, the error remains below 0.5%.

In Fig. 11, similar to the voltage, the maximum error occurs during the first transient, where it is 1.38%. Subsequently, it remains below 1%, including the peaks generated by the perturbations.

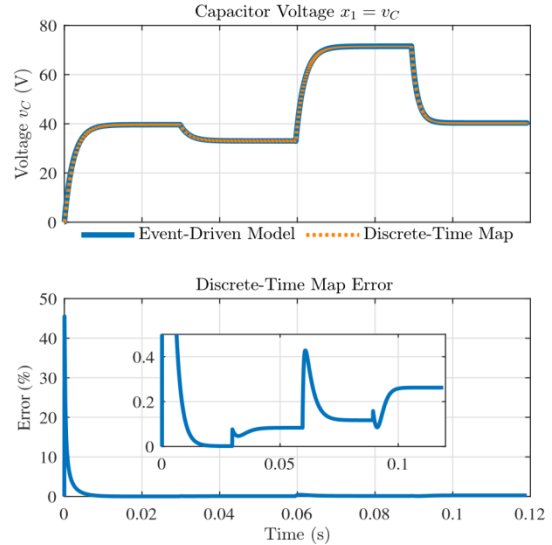


Fig. 10. Voltage response to disturbances.

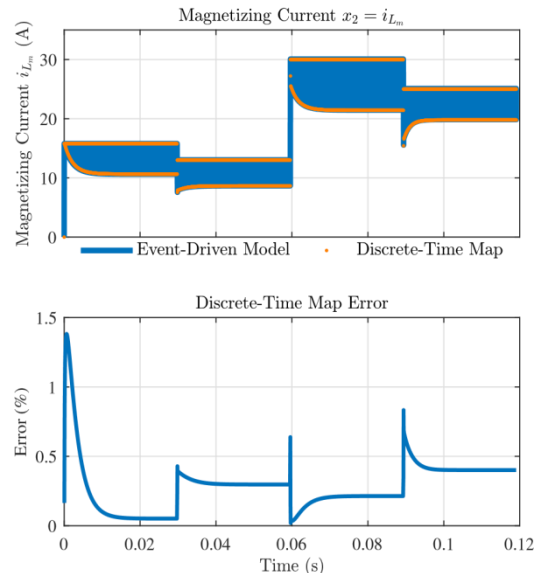


Fig. 11. Current response to disturbances.

### V. CONCLUSIONS AND FUTURE WORK

In this work, we have developed a discrete-time map for a flyback converter with peak current control based on the nonlinear averaged model, which has proven to be significantly more efficient in terms of simulation time compared to the event-driven model. The results showed a reduction in simulation time of approximately 97%, while maintaining adequate accuracy in both transient and steady-state conditions, with errors less than 1%.

The proposed method allows for the accurate identification of transitions between CCM and DCM. Additionally, results show that the map can track changes in the reference current quickly and accurately, efficiently adjusting to each new condition without compromising the stability of the system. This demonstrates the effectiveness

of the model in real-world operating scenarios where conditions can vary unexpectedly and abruptly.

This model can be integrated into different simulation environments, such as SPICE-based software or power system stability analysis tools. These integrations enable the detailed study of the behavior of multiple power converters connected to various nodes in a network, optimizing their operation and coordination within distributed generation systems.

The proposed model allows for quick and accurate evaluation of the system dynamics, making it suitable for use in renewable energy generation applications and scenarios where system response under different operating conditions must be analyzed. In addition, the simplified modeling approach helps reduce computational complexity, which is beneficial for large-scale simulations and the development of efficient control systems.

The proposed model has a limitation at very low frequencies due to the linear approximation of the current waveform, which becomes less accurate as the frequency decreases. Nevertheless, at higher frequencies, the model maintains high accuracy and computational efficiency. Future work will focus on addressing this limitation to further enhance the model's applicability across a broader frequency range.

As future work, it is proposed to validate the discrete-time map with different DC-DC converter topologies and implement additional control techniques that could further enhance system stability and efficiency. Furthermore, it would be interesting to explore the integration of the model into real-time simulation environments for microgrid and distributed energy system applications.

#### CONFLICT OF INTEREST

The authors declare no conflict of interest.

#### AUTHOR CONTRIBUTIONS

David E. Giraldo-Hernández (DEG-H), Mario A. Bolaños-Navarrete (MAB-N) and Gustavo Osorio (GO): Validation; Fabiola Angulo (FA): formal analysis; DEG-H, MAB-N, Nicols Astaiza (NA) and Juan David Mina-Casaran (JDM-C): investigation; DEG-H, MAB-N, FA, NA and JDM-C: original draft preparation; DEG-H, MAB-N, FA and GO; supervision, FA, GO and Wilder Herrera (WH): review and editing. All authors have read and agreed to the published version of the manuscript.

#### FUNDING

This work was supported by Universidad Nacional de Colombia, Rymel Ingenieria Eléctrica S.A.S. and Patrimonio Autónomo Fondo Nacional de Financiamiento para la Ciencia, la Tecnología y la Innovación Francisco José de Caldas - Ministerio de Ciencia, Tecnología e Innovación under the project "Validación tecnológica para la fabricación de reconectores automáticos para redes inteligentes, del tipo seco con polos encapsulados utilizando compuestos poliméricos termoestables", contract No. 099-2022.

#### REFERENCES

- [1] M. H. Rashid, *Power Electronics Handbook*, 5th ed., Butterworth-Heinemann, 2023.
- [2] J. L. Seguel, S. I. Seleme Jr, and L. M. Morais, "Comparative study of buck-boost, SEPIC, Cuk and Zeta DC-DC converters using different MPPT methods for photovoltaic applications," *Energies*, vol. 15, no. 21, #7936, 2022.
- [3] S. P. Litrán, E. Durán, J. Semiño, and C. Díaz-Martín, "Multiple-output DC-DC converters: applications and solutions," *Electronics*, vol. 11, no. 8, #1258, 2022.
- [4] J.-H. Choi, H.-M. Kwon, and J.-Y. Lee, "Design of a 3.3 kw/100 khz EV charger based on flyback converter with active snubber," *IEEE Trans. on Vehicular Technology*, vol. 71, no. 7, pp. 7161–7170, 2022.
- [5] C. A. Ramos-Paja, J. D. Bastidas-Rodríguez, and A. J. Saavedra-Montes, "Design and control of a battery charger/discharger based on the flyback topology," *Applied Sciences*, vol. 11, no. 22, #10506, 2021.
- [6] M. Ponce-Silva, D. Salazar-Pérez, O. M. Rodríguez-Benítez *et al.*, "Flyback converter for solid-state lighting applications with partial energy processing," *Electronics*, vol. 10, no. 1, #60, 2020.
- [7] C. Shah, J. D. Vasquez-Plaza, D. D. Campo-Ossa *et al.*, "Review of dynamic and transient modeling of power electronic converters for converter dominated power systems," *IEEE Access*, vol. 9, pp. 82094–82117, 2021.
- [8] Y. Gui, R. Han, J. M. Guerrero, J. C. Vasquez, B. Wei, and W. Kim, "Large-signal stability improvement of DC-DC converters in DC microgrid," *IEEE Trans. on Energy Conversion*, vol. 36, no. 3, pp. 2534–2544, Sep. 2021.
- [9] A. E. Aroudi, R. Haroun, M. Al-Numay, J. Calvente, and R. Giral, "A large-signal model for a peak current mode controlled boost converter with constant power loads," *IEEE Journal of Emerging and Selected Topics in Power Electronics*, vol. 9, no. 1, pp. 559–568, 2019.
- [10] L. Benadero, A. El Aroudi, L. Martínez-Salamero, and C. K. Tse, "In-depth analysis of smooth and nonsmooth bifurcations for an open-loop boost converter feeding constant power loads in discontinuous conduction mode," *International Journal of Bifurcation and Chaos*, vol. 33, no. 4, #2350043, 2023.
- [11] A. Nduwamungu, T. T. Lie, I. Lestas, N.-K. C. Nair, and K. Gunawardane, "Control strategies and stabilization techniques for DC/DC converters application in DC MGS: challenges, opportunities, and prospects—A review," *Energies*, vol. 17, no. 3, #669, 2024.
- [12] S. Howimanporn and C. Bunlaksanusorn, "Performance comparison of Continuous Conduction Mode (CCM) and discontinuous conduction mode (DCM) flyback converters," in *Proc. of the Fifth Int. Conf. on Power Electronics and Drive Systems*, 2003, vol. 2, pp. 1434–1438.
- [13] S. Zhou, G. Zhou, M. He, S. Mao, H. Zhao, and G. Liu, "Stability effect of different modulation parameters in voltage-mode PWM control for CCM switching DC-DC converter," *IEEE Trans. on Transportation Electrification*, vol. 10, no. 2, pp. 2408–2422, 2023.
- [14] A. El Aroudi, B. Robert, and L. Martínez-Salamero, "Modelling and analysis of multicell converters using discrete time models," in *Proc. of 2006 IEEE Int. Symp. on Circuits and Systems*, 2006. doi: 10.1109/ISCAS.2006.1693046
- [15] P. Iordanov and M. Halton, "Discrete-time modelling and robust analysis of a buck converter," *IFAC Proc. Volumes*, vol. 45, no. 13, pp. 647–652, 2012.
- [16] J. A. Baxter and D. J. Costinett, "Converter analysis using discrete time state-space modeling," in *Proc. of 2019 20th Workshop on Control and Modeling for Power Electronics*, 2019. doi: 10.1109/COMPEL.2019.8769686
- [17] W. Yuanbin, "Research on chaos in switching DC-DC converters," in *Proc. of 2009 Second Int. Conf. on Intelligent Computation Technology and Automation*, 2009, vol. 3, pp. 91–94.
- [18] Z. Xiao, W. Lei, G. Gao, H. Wang, and W. Mu, "Simplified discrete-time modeling for convenient stability prediction of DAB converter in energy storage system," *IEEE Trans. on Power Electronics*, vol. 39, no. 10, pp. 12636–12651, 2024.
- [19] M. Al-Numay, "Averaged discrete-time model for fast simulation of PWM converters in DCM," *International Journal of Modelling and Simulation*, vol. 29, no. 1, pp. 46–51, 2009.
- [20] C. Cheng, F. Xie, B. Zhang, D. Qiu, W. Xiao, and H. Ji, "Modeling

and nonlinear dynamic analysis of cascaded DC–DC converter systems based on simplified discrete mapping.” *IEEE Trans. on Industrial Electronics*, vol. 70, no. 6, pp. 5830–5839, 2022.

- [21] R. Dhifaou and H. Brahmi, “Fast simulation and chaos investigation of a DC–DC boost inverter,” *Complexity*, vol. 2021, no. 1, #9162259, 2021.
- [22] S. Bacha, I. Munteanu, and A. I. Bratcu, *Power Electronic Converters Modeling and Control*, Springer, 2014.
- [23] S. F. Graziani, T. V. Cook, and B. M. Grainger, “Isolated flying capacitor multilevel converters,” *IEEE Open Journal of Power Electronics*, vol. 3, pp. 197–208, 2022.
- [24] M. Forouzesh, Y. P. Siwakoti, S. A. Gorji, F. Blaabjerg, and B. Lehman, “Step-up DC–DC converters: A comprehensive review of voltage-boosting techniques, topologies, and applications,” *IEEE Trans. on Power Electronics*, vol. 32, no. 12, pp. 9143–9178, 2017.
- [25] D. W. Hart, *Electrónica de Potencia*, 1st ed. Prentice Hall, 2001.
- [26] M. H. Rashid, *Power Electronics: Devices, Circuits, and Applications*, 4th ed., Pearson, 2014.
- [27] F. Gokcegoz, E. Akboy, and A. H. Obdan, “Analysis and design of a flyback converter for universal input and wide load ranges,” *Electrica*, vol. 21, no. 2, pp. 235–241, 2021.

Copyright © 2025 by the authors. This is an open access article distributed under the Creative Commons Attribution License ([CC BY 4.0](https://creativecommons.org/licenses/by/4.0/)), which permits use, distribution and reproduction in any medium, provided that the article is properly cited, the use is non-commercial and no modifications or adaptations are made.



**David E. Giraldo-Hernández** received the B.S. degree in electronic engineering and the B.S. degree in electrical engineering from Universidad Nacional de Colombia, sede Manizales, Colombia, in 2023 and 2024, respectively. Currently, he is pursuing the M.Sc. degree in industrial automation at Universidad Nacional de Colombia, sede Manizales, Colombia. His research interests include nonlinear control, nonlinear dynamics,

renewable systems, power converters, and applications to dc-dc converters. He is a member of the research group Perception and Intelligent Control (PCI).



**Mario A. Bolaños-Navarrete** received the electronic engineering degree and the master’s degree in industrial automation from Universidad Nacional de Colombia in 2012 and 2016, respectively. He is currently pursuing the Ph.D. degree at Universidad Nacional de Colombia. He has worked as a lecturer and researcher in topics related to power converters. He is currently a member of the Percepción y Control Inteligente (PCI)

research group at Universidad Nacional de Colombia, Manizales. His main research interests include power converters, inverters, power electronics, distributed generation, and sliding mode control.



**Fabiola Angulo** received the B.S. degree in electrical engineering (with honors) from Universidad Nacional de Colombia, sede de Manizales, Colombia, and the Ph.D. degree in automatics and robotics from the Technical University of Catalonia (UPC), Barcelona, Spain, in 1989, 2000, and 2004, respectively. She is currently a full professor in the Department of Electrical Engineering, Electronics and Computer Science. Her research interests include nonlinear control,

nonlinear dynamics of nonsmooth systems, and applications to dc-dc converters. She is member of the research group Perception and Intelligent Control (PCI), and Head of many applied research projects.



**Gustavo Osorio** has received the degree in electronic engineering in 1997 and M.Eng. in industrial automation in 2003 from the Universidad Nacional de Colombia Sede Manizales. In 2008 he received his PhD in computer and control engineering from the Università degli Studi di Napoli Federico II (Italy). He has been at the Department on Electric, Electronic and Computing Engineering at the Universidad Nacional de Colombia sede Manizales since 1998 as an assistant instructor. In 2013 he became titular professor and his research interests include dynamical and control systems, computer engineering and electronic circuits design.



**Jhoselin N. Astaiza** received his B.S. degree in electronic engineering from Universidad del Valle, Cali, Colombia, in 2022, and her specialization in Project Management from Universidad EAFIT, Medellín, Colombia, in 2024. She works as a researcher in the Research and Development area at RYMEL Ingeniería Eléctrica S.A.S., Copacabana, and currently works in the Rymel Innovation Group (RYNOVA). Her main research interests include renewable systems, electrical instrument transformers and electrical testing of transformers.

instrument transformers and electrical testing of transformers.



**Juan D. Mina-Casaran** received the degree, M.Sc., and Ph.D. degrees in electrical engineering from Universidad del Valle, Cali, Colombia, in 2013, 2016, and 2022, respectively. He performs as a Research and Development Director with RYMEL Ingeniería Eléctrica S.A.S., Copacabana, Colombia, and is currently working with the Rymel Innovation Group (RYNOVA). His main research interests include power system

planning, electrical transformers and analysis and modeling of electrical phenomena.



**Wilder Herrera** received his B.Sc. degree in electrical engineering from Universidad del Valle, Cali, Colombia, in 2009, and his Ph.D. degree in electrical engineering from the same institution in 2014. He is currently the research leader of the Rynova Research Group. His work focuses on the design, modeling, and diagnosis of distribution transformers and electrical equipment for medium-voltage lines, as well as the research and application of new materials for the manufacturing of electrical

equipment. Under his leadership, the Rynova Research Group has established partnerships with academic institutions and industrial organizations to promote knowledge transfer and foster innovation.